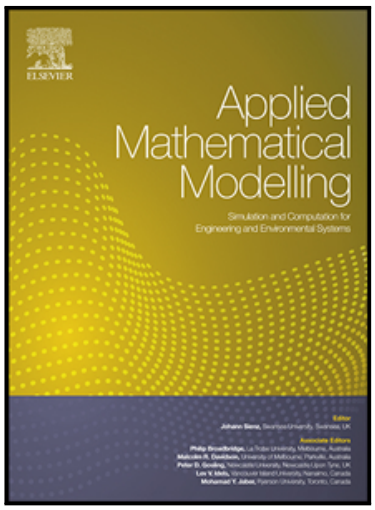

A coupled NMM-SPH method for fluid-structure interaction problems

Ying Xu , Changyi Yu , Feng Liu , Qinya Liu

PII: S0307-904X(19)30382-8
DOI: https://doi.org/10.1016/j.apm.2019.06.020
Reference: APM 12888

To appear in: *Applied Mathematical Modelling*

Received date: 1 December 2018
Revised date: 9 June 2019
Accepted date: 17 June 2019

Please cite this article as: Ying Xu , Changyi Yu , Feng Liu , Qinya Liu , A coupled NMM-SPH method for fluid-structure interaction problems, *Applied Mathematical Modelling* (2019), doi: https://doi.org/10.1016/j.apm.2019.06.020

Highlights

- A coupled NMM-SPH method for fluid-structure interaction problems is present.
- The proposed method takes full advantage of NMM for the solid structures and SPH for fluid particles.
- A contact algorithm is developed which can handle the interaction between NMM elements and SPH particles well.
- Compared to DDA-SPH or DEM-SPH, NMM-SPH can accurately calculate the stress of the structure.
- The proposed method can also predict the failure of the solid structure under the action of fluid.

A coupled NMM-SPH method for fluid-structure interaction problems

Ying Xu[1], Changyi Yu[2, 3, 4], Feng Liu[1, 5*], Qinya Liu[6]

[1]*State Key Laboratory of Hydraulic Engineering Simulation and Safety, School of Civil Engineering, Tianjin University, Tianjin 300072, China*

[2]*CCCC-Tianjin Port Engineering Institute, Co. Ltd., Tianjin 300222, China*

[3]*CCCC First Harbor Engineering Company, Co. Ltd., Tianjin 300461, China*

[4]*Key Laboratory of Geotechnical Engineering of Tianjin, Tianjin 300222, China*

[5]*State Key Laboratory of Geomechanics and Geotechnical Engineering, Institute of Rock and Soil Mechanics, Chinese Academy of Sciences, Wuhan 430071, China*

[6]*Department of Physics, University of Toronto, ON, Canada M5S 1A7*

Abstract: The main challenges in the numerical simulation of fluid–structure interaction (FSI) problems include the solid fracture, the free surface fluid flow, and the interactions between the solid and the fluid. Aiming to improve the treatment of these issues, a new coupled scheme is developed in this paper. For the solid structure, the Numerical Manifold Method (NMM) is adopted, in which the solid is allowed to change from continuum to discontinuum. The Smoothed Particle Hydrodynamics (SPH) method, which is suitable for free interface flow problem, is used to model the motion of fluids. A contact algorithm is then developed to handle the interaction between NMM elements and SPH particles. Three numerical examples are tested to validate the coupled NMM-SPH method, including the hydrostatic pressure test, dam-break simulation and crack propagation of a gravity dam under hydraulic pressure. Numerical modelling results indicate that the coupled NMM-SPH method

can not only simulate the interaction of the solid structure and the fluid as in conventional methods, but also can predict the failure of the solid structure.

Keywords: Fluid–structure interaction, Numerical manifold method, Smoothed Particle Hydrodynamics, Coupled NMM-SPH method, contact algorithm

1. Introduction

Fluid–structure interaction (FSI) is the interaction of a movable or deformable structure with an internal or surrounding fluid flow. FSI therefore involves the theoretical coupling between fluid dynamics and structural mechanics [1]. Specifically, the structure suffers pressure from the fluid flow to give rise to deformation and movement; conversely, the fluid pressure field and flow is affected by the moveable or deformable structure.

FSI is a common phenomenon in many engineering systems and processes, such as aircraft and naval architecture, dam failure, and landslide-induced waves. FSI problems usually involve multiphysics couplings that are almost impossible to be solve by analytical methods. Although a few numerical methods have been developed for FSI problems, most of them can only simulate the individual response of the fluid or the structure [2]. Actually, it is difficult to simulate both the structure and the fluid using a single numerical method. A coupled method is an obvious solution, but the development of coupled methods is still limited.

For fluid dynamic problems, Smoothed Particle Hydrodynamics (SPH) [3] is an

excellent method and has been frequently used, especially for problems involving free interface flow [4]. As one of the earliest meshfree methods, SPH is a pure Lagrangian method. In the SPH method, the matter (air, fluid or continuum media) is treated as a set of discretized particles. Each particle possesses several physical quantities including position, density, pressure, and velocity. Since the particles are independent when they are separated by more than the smoothing length, SPH can easily capture large interface deformation, breaking, merging and splashing phenomenon. SPH is thus suitable for the simulation of free surface of fluid [5], two- and three-phase flow [6, 7]. With the advances of computer power, SPH has been applied to the simulation of many real engineering problems [8], even large-scale engineering problems with more than 10^9 particles [9].

For solid mechanics problems, the finite element method (FEM) is one of the most widely used numerical methods. It is possible to couple FEM with SPH to solve FIS problems [10-12]. The coupled FEM-SPH method has the capability of performing complex seakeeping analyses coupled with highly nonlinear internal flows within reasonable computational time. However, it is difficult for FEM to handle large translations, rotations, and contacts. Another common method for simulating solids deformation is the Discrete Element Method (DEM). DEM has also been used to couple with SPH for FSI problems. Cleary [13, 14] used a coupled DEM-SPH to predict the motion of the solid particles interacting with slurry flow. Moreover, Wu et al. [2] studied FSI problems with fracture in the structure induced by the free surface flow of the fluid. However, DEM requires the introduction of artificial damping to achieve the computational stability. Recently,

Discontinuous Deformation Analysis (DDA) was coupled with SPH to analyze landslide-generated impulsive waves [15, 16] . The major advantage of DDA is the simulation of the motion of blocks with arbitrary shapes without introducing artificial damping. However, DDA cannot accurately capture the deformation and stress of the structure.

The Numerical Manifold Method (NMM) proposed by Shi [17, 18] combines the advantages of both the continuum-based FEM and the discontinuum-based DDA through two cover systems. NMM inherits not only the advantages of FEM in accurately calculating the stress and strain fields, but also the advantages of DDA in dealing with discrete systems. The meshes in NMM do not need to coincide with the crack face and material boundary, which makes NMM a very suitable numerical method for solving problems with complex geometrical boundaries. Due to these unique features, NMM has been applied to solve various engineering problems, such as the crack propagation problem [19, 20], stress wave propagation [21], seepage flow analysis in porous media [22], thin plate problems [23], and hydraulic fracture problems [24].

In this study, a coupled NMM-SPH is proposed for FSI problems for the first time, where NMM describes the deformation, movement and fracture of the solid structure while SPH solves the fluid flow. The coupled NMM-SPH method inherits the above mentioned advantages for its both parental methods. The main goal of the present paper is to establish the coupled NMM-SPH method and to validate its effectiveness. More complex FSI problems will be considered in future work.

This paper is organized as follows. The basic concepts of SPH and NMM are briefly introduced in Section 2 and 3, respectively. Section 4 details the NMM-SPH coupling scheme. Numerical examples are presented in Section 5 and Section 6 concludes the entire paper.

2. SPH method

Since it was proposed in the 1970s, SPH has made great progress in both theory and application. Here we only give a brief introduction of SPH and more details can be found in the literature [25].

2.1 Kernel approximation

In the SPH method, the entire material domain is represented by a finite number of particles that carry certain mass and occupy certain space. The discretization of the governing equations is based on these discrete particles. Using these particles, a function and its derivatives are evaluated on the particles through a kernel approximation. The kernel approximation of a function $f(\boldsymbol{x})$ can be written as,

$$f(\boldsymbol{x}) \approx \int_{\Omega} f(\boldsymbol{x}')\, W(\boldsymbol{x}-\boldsymbol{x}', h) dx' \tag{1}$$

where f is a function of the position vector $\boldsymbol{x}$, $\mathrm{W}(\boldsymbol{x}-\boldsymbol{x}', h)$ is the smoothing kernel function or kernel function, and h is the smoothing length defining the influence zone of W.

The continuous integral representations concerning the SPH kernel approximation can be represented by discretized forms of summation over all the particles in the support domain, as shown in Fig. 1. This discretization process of summation over the particles is commonly known as particle approximation in the SPH literature.

The kernel function W should satisfy a few conditions, such as unity condition, Delta function property and compact condition. Many kernel functions have been proposed in the literature [25]. In this paper, the modified Gaussian function is adopted as the smoothing kernel [26],

$$\mathrm{W}(\boldsymbol{x}) = \frac{e^{-\left(\frac{|x|}{kh}\right)^2} - e^{-\left(\frac{\delta_c}{kh}\right)^2}}{2\pi \int_0^{\delta_c} S\left(e^{-\left(\frac{S}{kh}\right)^2} - e^{-\left(\frac{\delta_c}{kh}\right)^2}\right) dS} \tag{2}$$

where δ_c is a cut-off distance, which is introduced to satisfy the compact condition, and S is the distance from point x to a certain particle.

The smoothing length in the kernel function is an important parameter, which determines the influence range of particles. Larger smoothing length means that the response at one particle is influenced by more neighboring particles. Thus, the smoothing length can significantly affect the computational accuracy and efficiency. To achieve symmetry of the interactions between particles, the smoothing length can be computed by

$$h_{ij} = \frac{h_i + h_j}{2} \tag{3}$$

Alternatively, the symmetry of the interactions can also be achieved with the help of the kernel function by

$$W_{ij} = \frac{1}{2}\left(W(h_i) + W\left(h_j\right)\right) \tag{4}$$

2.2 Governing equations

The governing equations for dynamic fluid flows are the well-known Navier-Stokes (N-S) equations, which include the conservation of mass and momentum. By applying

particle discretization and the above kernel approximation, the N-S equations can be rewritten in the SPH notation as [25],

$$\frac{D\rho_i}{dt} = \rho_i \sum_{j=1}^{N} \frac{m_j}{\rho_j} \boldsymbol{v}_{ij} \cdot \frac{\partial W_{ij}}{\partial \boldsymbol{x_i}} \tag{5}$$

$$\frac{D\boldsymbol{v}_i}{dt} = \sum_{j=1}^{N} m_j \frac{\sigma_i + \sigma_j}{\rho_i \rho_j} \frac{\partial W_{ij}}{\partial \boldsymbol{x_i}} \tag{6}$$

where ρ is the density; N is the number of particles in the support domain of particle i; m_j is the mass associated with particle j; $\boldsymbol{v}_{ij} = \boldsymbol{v}_i - \boldsymbol{v}_j$ with $\boldsymbol{v}$ the velocity of particles, $W_{ij} = W(\boldsymbol{x}_i - \boldsymbol{x}_j, h) = W(|\boldsymbol{x}_i - \boldsymbol{x}_j|, h) = W(R_{ij}, h)$, σ is the total stress tensor, which is composed of two parts, the isotropic pressure and viscous stress [25]. W_{ij} is the smoothing function of particle i evaluated at particle j, and is closely related to the smoothing length h.

In the SPH method, pressure term can be solved by the Equation of State (EoS), and one of frequently-used EoS is given by Monaghan [27]:

$$P = \frac{\rho_0 C_0^2}{\gamma} \left[\left(\frac{\rho}{\rho_0} \right)^{\gamma} - 1 \right] \tag{7}$$

where ρ_0 is the reference density; γ is a constant taken to be 7 for water [28-31], 1.4 for air [32]. C_0 is the sound velocity based on the Mach number. It should be noted that the larger the value of C_0 is, the smaller the value of permissible time step Δt. Hence, to avoid the unnecessary increase in the computational time, C_0 should be small enough while guaranteeing the incompressibility condition [29]. C_0 can be obtained by the method presented in the literature [33].

3. NMM method

Since, the background and basic theory of NMM have been described in great details in

the literature [19, 20, 34, 35], here we only give a brief introduction.

By using dual cover systems, namely the mathematical cover (MC) and physical cover (PC), NMM provides a unified framework for both continuous and discontinuous problems. MC is composed of a set of simply-connected domains, each of which is called a mathematical patch (MP). The MP does not need to coincide with the problem domain Ω, as long as all the MPs together can cover Ω completely. Physical patches (PPs) are obtained by the intersection of each MP and Ω. All the PPs together make up the PC. It can be seen that PC relies on the physical features of Ω. Then a manifold element (ME) can be formed by the common area of several adjacent PPs. MEs can be either convex or concave polygons.

Fig. 2 is an example demonstrating the cover systems in NMM, where the problem domain Ω containing the crack Γ is covered by three mathematical patches, rectangle M_1, rectangle M_2 and circle M_3. By the intersection operation between MPs and Ω, PPs are obtained. For example, P_1 is generated from M_1, P_2 and P_3 from M_2, P_4 from M_3, as shown in Fig. 3. It is clear that for one MP, more than one PP can be generated. Simply connected PPs containing no crack tip are called nonsingular patches, such as P_4, while a physical patch containing at least one crack tip is called a singular patch, such as P_1. The overlap of adjacent PPs forms the Manifold Element (ME). At last, nine MEs are generated as shown in Fig. 4. For example, E_1 covered by P_1, E_2 covered by P_1 and P_2, E_4 covered by P_1, P_2 and P_4.

The integration over MEs in NMM is accomplished by the simplex integration method. This integration method can be implemented on any shape without Gauss integration points when the integrand is polynomial [17, 36].

A cover function (also termed a local approximation function) is defined over each PP. On each ME, the displacement can be expressed using the cover function as:

$$u^h(\boldsymbol{x}) = \sum_{i=1}^{n} w_i(\boldsymbol{x}) u_i^h(\boldsymbol{x}) \tag{8}$$

where n is the number of PP that cover present ME, $u_i^h(\boldsymbol{x})$ is the value of cover function of the i-th PP at position $\boldsymbol{x}$, $w_i(\boldsymbol{x})$ is the weight function of the i-th PP. All the weight functions $w_i(\boldsymbol{x})$ constitute the partition of unity. If the FE-based cover systems are adopted, the weight function is identified as the shape function in FEM.

The most convenient way to construct cover function is to use the polynomial basis. However, for singular patches, polynomial cover function may lead to a poor approximation of the solution. In such cases, prior known knowledge about the solution, such as Williams' series of the crack tip, can be adopted to construct the cover function [19]. For convenience, in this work the constant basis is adopted, which means that each physical patch has two degrees of freedom.

Given Equation (8), with the help of minimum potential principle or principle of virtual work, the discrete equations for a dynamic analysis can be obtained [35].

4. NMM-SPH coupling strategy

In the SPH method, it is essential to deal with the interaction between boundaries and fluid particles. There are several existing strategies to do that. The first one is that the particles locating at the coupling interface are adsorbed on the FEM nodes [37, 38]. This algorithm was used for simulating consistent deformation of the solid and the fluid. It is

however not suitable for large deformation problems such as dam break problem. In the second method, the contact is judged by the distance between a particle and a line [39-41]. This algorithm is readily understandable and applicable for FSI problems with large deformation. However, this method is computationally expensive and has significant truncation error in the boundary region. Another approach is to place virtual particles on and inside the solid boundary [25]. But this method can cause significant errors at sharp corners, where virtual particles overlap with each other. To address this issue, Wang [15] introduced only boundary particles in coupled DDA-SPH method. A similar contact algorithm is proposed in this paper for NMM.

In the SPH method, a region is determined as the computational domain, as shown in Fig. 5. Virtual particles are arranged on the NMM boundaries that are inside or intersect with the computational domain. Because the virtual particles are only needed along the boundaries, this new schemes can reduce the computing time compared with the method in [25].

In Fig. 5, boundary FG locates inside the computational domain, while boundaries AB、BC、EF and GH intersect with the computational domain. Virtual particles occupy the entire boundary because the domain of influence of real particles can exceed the computational domain. It is worth noting that the distance between two virtual particles is not the Euclidean distance, it is the distance along the boundaries, see Fig. 6. This strategy guarantees reasonable layout of virtual particles even for sharp corners.

In the coupled NMM-SPH method, the position and velocity of virtual particles are influenced by NMM boundaries, while SPH particles apply force to NMM boundaries. The

interaction scheme between the fluid particles and solid boundaries in the coupled NMM-SPH method is shown in Fig. 7.

To consider the interaction between the particles and the blocks, the interaction force is taken as the point load at the boundary particles that is perpendicular to the solid surface. The main advantage of this treatment is that there is no need to deal with complex pressure fields. Further it does not require an integral pressure field. All the interaction forces are applied as the point loading.

The next step is to calculate the magnitude of the interaction force. In the coupled DDA-SPH method, the standardized "penalty-force" [42] method was adopted. In present paper, the interaction force is calculated using the pressure of neighboring fluid particles. The steps are as follows:

(1) Compute the pressure of virtual particles using the pressure of neighboring fluid particles, as shown in Fig. 8,

$$P_i = \frac{\sum_j P_j W_{ij}}{\sum_j W_{ij}} \tag{9}$$

where P_j is the pressure of neighboring fluid particle j, W is the weight function.

(2) Calculate the interaction point loading with the pressure,

$$\boldsymbol{F}_i = P_i * h \tag{10}$$

where h is the initial spacing of real particles.

Up to now, the point loading can be completely determined. The computation procedure of the coupled NMM-SPH method in a single loop is illustrated in Fig. 9.

In both NMM and SPH methods, a proper time step is needed to implement the time

integration. After obtaining two time steps separately, the smaller one is selected as the time step for the coupled method.

5. Numerical examples

5.1 Hydrostatic pressure test

To verify the proposed coupling strategy, the hydrostatic pressure in a tank is first tested. As shown in Fig. 10, the internal height and width of the water tank are 0.5 m, the thickness of the tank is 0.1 m, and the depth of the water is 0.48 m. The computational parameters are as follows: the density of water is 1000 kg/m^3, the acceleration of gravity is 9.8 m/s^2. The particle spacing is set to be 0.02 m, resulting in a total number of 576 fluid particles. The time step is set to 10^{-4} s and the total computational time is 1.1 s when the computation is completely stable.

The final configuration and hydrostatic pressure are shown in Fig. 11. From the stable positions of particles, the computational accuracy near the boundary, especially at the corner, is slightly lower than that in inner regions. According to the hydrostatics theory, the pressure of the tank bottom is 4704 Pa and the point loading of each particle at the tank bottom is 94.08 N. The results from NMM-SPH are plotted in Fig. 12, where Fig. 12a shows the pressure of fluid particles locating at the left, right and bottom; Fig. 12b shows the point loading of virtual particles at the internal boundaries. The relative errors are less than 0.7%. This example proves that the proposed contact algorithm is effective and accurate, and the proposed coupling strategy can handle the interaction of solid and fluid properly.

5.2. Dam break simulation

The dam break problem is often considered in the SPH literature [43-47] to show the ability of SPH models to deal with large deformation of the interface. In general, the boundaries of this problem are fixed and non-deformable. In the coupled NMM-SPH method however, both the deformation and the stress of the dam can be obtained.

Fig. 13 shows a sketch of the initial setup for the dam break [26, 33], where L/H = 2, D/H = 3, d/H = 5.366. Particles are initially positioned on a Cartesian lattice with the resolution of 50×100. The solution has been integrated in time by leapfrog integration scheme with time step 4×10^{-4}s. The pressure field is initialized with an approximate solution of the Laplace problem, where the pressure is zero at the free surface (the top and the right sides of the fluid domain).

Under the action of gravity, the water column collapses (in Fig. 14(a)) and propagates along the floor (in Fig. 14 (b)). Then, the fluid impacts the vertical wall of right-hand side. A vertical jet grows up, overturns backward and then falls down (in Fig. 14(c)). Finally, the fluid impacts the left-hand side vertical wall (in Fig.14(d)).

Comparing to the results in literatures [26, 45], the water impact height of this paper is slightly lower than that in the literature when fluid impacts the right-hand side vertical wall. This is because that the wall is elastic and it can deform and absorb part of the kinetic energy of the flow when impacted by the fluid. The particle regularized density strategy [48] is used to improve the accuracy of the fluid. The surface of the fluid is smoother and more stable. During the impact, the fluid maintains integrity without splash.

5.3. Crack propagation of Koyna Dam

This case demonstrates the potential ability of the coupled NMM-SPH method to predict solid structure failure under the impact of fluid. Koyna Dam is selected as a practical example.

The initial configuration with a short crack is illustrated in Fig. 15. For the sake of convenience, the crack tip is restricted on the boundaries of manifold elements throughout the computational process. The parameters of the dam are as follows, Young's modulus E=35 GP, Poisson's ratio v=0.25. The Mohr-Coulomb strength criterion with tension cutoff [49] is used for crack propagation, where tension strength t_0=3 MPa, cohesion C=10 MPa, and frictional angle φ=50°. The density of water is 1000 kg/m^2.

The initial NMM mesh and SPH particles are shown in Fig. 16. The hydraulic pressure, also shown in Fig. 16, remained relatively stable during the process. To analyze the failure of the dam, we here pay more attention to the stress state of the dam. With the help of NMM, the stress of the dam can be easily evaluated at any time step. Under the action of hydraulic pressure, the crack will propagate towards the dam foundation leading to the failure of the entire dam. The crack paths predicted by the proposed coupled method and the stress in the x-direction at different steps are plotted in Fig. 17. It is found that the crack propagation is mainly caused by tension failure.

It should be noted that, in this example, the crack opening is too small to let the SPH particles move in. But if the crack opening is large enough, the SPH particles can move into the crack gap and exert pressure to the crack surfaces.

6. Conclusion

In this study, a coupled NMM-SPH method was developed for FSI problems. The fluid is discretized into particles in the SPH method, while the solid is modeled by the NMM method. A contact algorithm fitted for NMM-SPH method is designed to consider the interaction of the fluid and the solid.

The coupled NMM-SPH method is verified by three examples. In the hydrostatic pressure test, the results demonstrate excellent accuracy in comparison with the analytical solution, which illustrates the effectiveness of the proposed contact algorithm. The second dam break example proves the potential of NMM-SPH for simulating free surfaces problems. In the third example, NMM-SPH could even simulate the fracture of the solid structure under hydrostatic pressure. This makes NMM-SPH a suitable method for a wider range of FSI applications.

Inheriting merits of NMM, the coupled NMM-SPH method has advantages over other coupled methods. Compared to the coupled FEM-SPH, NMM-SPH works better for problems involving large movement and discontinuous deformation. Compared to the coupled DEM-SPH or DDA-SPH method, NMM-SPH can calculate the stress of the solid with better accuracy. This feature is vital when considering the failure of the solid.

This paper shall be considered as a preliminary study of the coupled NMM-SPH method. It is believed that the NMM-SPH can be used to solve more complex problems, such as landslide-generated impulsive waves, and the process of dam break under fluid impact.

Acknowledgments

This work was supported by the National Key R&D Program of China (Grant No. 2018YFC0406800), the Natural Science Foundation of China (Grant No. 11602165, 51704211), and Supported by Open Research Fund of State Key Laboratory of Geomechanics and Geotechnical Engineering, Institute of Rock and Soil Mechanics, Chinese Academy of Sciences (Grant No. Z015010).

References

[1] COMSOL Inc. COMSOL Multiphysics User's guide2010.

[2] Wu K, Yang D, Wright N. A coupled SPH-DEM model for fluid-structure interaction problems with free-surface flow and structural failure. Computers & Structures 2016;177: 141-61.

[3] Gingold RA, Monaghan JJ. Smoothed particle hydrodynamics: theory and application to non-spherical stars. Monthly notices of the royal astronomical society 1977;181(3): 375-89.

[4] Shadloo MS, Oger G, Le Touzé D. Smoothed particle hydrodynamics method for fluid flows, towards industrial applications: Motivations, current state, and challenges. Computers & Fluids 2016;136: 11-34.

[5] Niu X, Yu J. A Modified SPH Model for Simulating Water Surface Waves. Procedia Engineering 2015;116: 254-61.

[6] Pahar G, Dhar A. Mixed miscible-immiscible fluid flow modelling with incompressible SPH framework. Engineering Analysis with Boundary Elements 2016;73: 50-60.

[7] Tartakovsky AM, Panchenko A. Pairwise Force Smoothed Particle Hydrodynamics model for multiphase flow: Surface tension and contact line dynamics. Journal of Computational Physics 2016;305: 1119-46.

[8] Ulrich C, Leonardi M, Rung T. Multi-physics SPH simulation of complex marine-engineering hydrodynamic problems. Ocean Engineering 2013;64: 109-21.

[9] Domínguez JM, Crespo AJC, Valdez-Balderas D, Rogers BD, Gómez-Gesteira M. New multi-GPU implementation for smoothed particle hydrodynamics on heterogeneous clusters. Computer Physics Communications 2013;184(8): 1848-60.

[10] Fourey G, Oger G, Le Touzé D, Alessandrini B. Violent Fluid-Structure Interaction simulations using a coupled SPH/FEM method. IOP Conference Series: Materials Science and Engineering 2010;10: 012041.

[11] Serván-Camas B, Cercós-Pita JL, Colom-Cobb J, García-Espinosa J, Souto-Iglesias A. Time domain simulation of coupled sloshing–seakeeping problems by SPH–FEM coupling. Ocean Engineering 2016;123: 383-96.

[12] Yang Q, Jones V, McCue L. Free-surface flow interactions with deformable structures using an SPH–FEM model. Ocean Engineering 2012;55: 136-47.

[13] Cleary PW. Prediction of coupled particle and fluid flows using DEM and SPH. Minerals Engineering 2015;73: 85-99.

[14] Cleary PW, Sinnott MD. Computational prediction of performance for a full scale Isamill: Part 2 – Wet models of charge and slurry transport. Minerals Engineering 2015;79: 239-60.

[15] Wang W, Chen G-q, Zhang H, Zhou S-h, Liu S-g, Wu Y-q, et al. Analysis of landslide-generated impulsive waves using a coupled DDA-SPH method. Engineering Analysis with Boundary Elements 2016;64: 267-77.

[16] Zhang H, Chen G, Zheng L, Zhang Y, Wu Y, Han Z, et al. A new discontinuous model for three dimensional analysis of fluid-solid interaction behaviour. Proceedings of the TC105 ISSMGE international symposium on geomechanics from micro to macro, Cambridge, UK2014. 503-08.

[17] Genhua S. Manifold method of material analysis. Transactions of the Ninth Army Conference on Applied Mathematics and Computing: Minneapolish, Minncsoda, USA; 1992. 51-76.

[18] Genhua S. Manifold method. Berkeley, California (USA): Tsi Press; 1996. 52-262.

[19] Zheng H, Liu F, Li CG. The MLS-based numerical manifold method with applications to crack analysis. International Journal of Fracture 2014;190(1-2): 147-66.

[20] Zheng H, Xu D. New strategies for some issues of numerical manifold method in simulation of crack propagation. International Journal for Numerical Methods in Engineering 2014;97(13): 986-1010.

[21] Zhao GF, Zhao XB, Zhu JB. Application of the numerical manifold method for stress wave propagation across rock masses. International Journal for Numerical & Analytical Methods in Geomechanics 2014;38(1): 92–110.

[22] Zheng H, Liu F, Li CG. Primal mixed solution to unconfined seepage flow in porous media with numerical manifold method. Appl Math Model 2015;39(2): 794-808.

[23] Zheng H, Liu ZJ, Ge XR. Numerical manifold space of Hermitian form and application to Kirchhoff's thin plate problems. International Journal for Numerical Methods in Engineering 2013;95(9): 721-39.

[24] Yang YT, Tang XH, Zheng H, Liu QS, Liu ZJ. Hydraulic fracturing modeling using the enriched numerical manifold method. Appl Math Model 2018;53: 462-86.

[25] Liu G-R, Liu MB. Smoothed particle hydrodynamics: a meshfree particle method: World Scientific; 2003.

[26] Cherfils JM, Pinon G, Rivoalen E. JOSEPHINE: A parallel SPH code for free-surface flows. Computer Physics Communications 2012;183(7): 1468-80.

[27] Monaghan J, Kos A. Solitary waves on a Cretan beach. Journal of waterway, port, coastal, and ocean engineering 1999;125(3): 145-55.

[28] Vorobyev A, Kriventsev V, Maschek W. Simulation of central sloshing experiments with smoothed particle hydrodynamics (SPH) method. Nuclear Engineering and Design 2011;241(8): 3086-96.

[29] Ozbulut M, Yildiz M, Goren O. A numerical investigation into the correction algorithms for SPH method in modeling violent free surface flows. International Journal of Mechanical Sciences 2014;79: 56-65.

[30] Khanpour M, Zarrati AR, Kolahdoozan M, Shakibaeinia A, Amirshahi SM. Mesh-free SPH modeling of sediment scouring and flushing. Computers & Fluids 2016;129: 67-78.

[31] Xu X. An improved SPH approach for simulating 3D dam-break flows with breaking waves. Computer Methods in Applied Mechanics and Engineering 2016;311: 723-42.

[32] Yan R, Monaghan JJ, Valizadeh A, Xu F. The effect of air on solid body impact with water in two dimensions. Journal of Fluids and Structures 2015;59: 146-64.

[33] Colagrossi A, Landrini M. Numerical simulation of interfacial flows by smoothed particle hydrodynamics. Journal of Computational Physics 2003;191(2): 448-75.

[34] Liu F, Yu C, Yang Y. An edge-based smoothed numerical manifold method and its application to static, free and forced vibration analyses. Engineering Analysis with Boundary Elements 2017.

[35] Ma GW, An XM, He L. The Numerical Manifold Method: A Review. International Journal of Computational Methods 2010;07(01): 1-32.

[36] Zeng W, Li J, Kang F. Numerical Manifold Method with Endochronic Theory for Elastoplasticity Analysis. Mathematical Problems in Engineering 2014;2014: 1-11.

[37] Jun-xiang XUX-lLIU. Analysis of structural response under blast loads using the coupled SPH-FEM approach. Journal of Zhejiang University-SCIENCE A 2008;9(9): 1184-92.

[38] De'an H, Chunhan L, YiHua X, Xu H. Analysis of explosion in concrete by axisymmetric FE-SPH adaptive coupling method. Engineering Computations 2014;31(4): 758-74.

[39] Hu D, Long T, Xiao Y, Han X, Gu Y. Fluid–structure interaction analysis by coupled FE–SPH model based on a novel searching algorithm. Computer Methods in Applied Mechanics and Engineering 2014;276: 266-86.

[40] Liu X, Liu S, Ji H. Numerical research on rock breaking performance of water jet based on SPH. Powder Technology 2015;286: 181-92.

[41] Long T, Hu D, Yang G, Wan D. A particle-element contact algorithm incorporated into the coupling methods of FEM-ISPH and FEM-WCSPH for FSI problems. Ocean Engineering 2016;123: 154-63.

[42] Mikola R, Sitar N. Next generation discontinuous rock mass models: 3-D and rock-fluid interaction. Frontiers of Discontinuous Numerical Methods and Practical Simulations in Engineering and Disaster Prevention 2013: 81-90.

[43] Xu X, Deng X-L. An improved weakly compressible SPH method for simulating free surface flows of viscous and viscoelastic fluids. Computer Physics Communications 2016;201: 43-62.

[44] Liu X, Xu H, Shao S, Lin P. An improved incompressible SPH model for simulation of wave–structure interaction. Computers & Fluids 2013;71: 113-23.

[45] Rouzbahani F, Hejranfar K. A truly incompressible smoothed particle hydrodynamics based on artificial compressibility method. Computer Physics Communications 2017;210: 10-28.

[46] Eslamian A, Khayat M. Numerical studies to propose a ghost particle removed SPH (GR-SPH) method. Appl Math Model 2017;42: 71-99.

[47] Lee ES, Moulinec C, Xu R, Violeau D, Laurence D, Stansby P. Comparisons of weakly compressible and truly incompressible algorithms for the SPH mesh free particle method. Journal of Computational Physics 2008;227(18): 8417-36.

[48] Liu MB, Xie WP, Liu GR. Modeling incompressible flows using a finite particle method. Appl Math Model 2005;29(12): 1252-70.

[49] Wu Z, Wong LNY. Frictional crack initiation and propagation analysis using the numerical manifold method. Computers and Geotechnics 2012;39: 38-53.

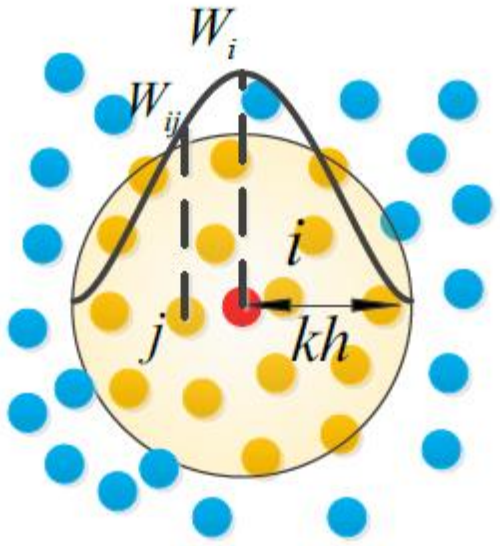

Fig. 1. Particle approximations using particles within the support domain of the kernel function W for particle i. The support domain is a circular with a radius of kh.

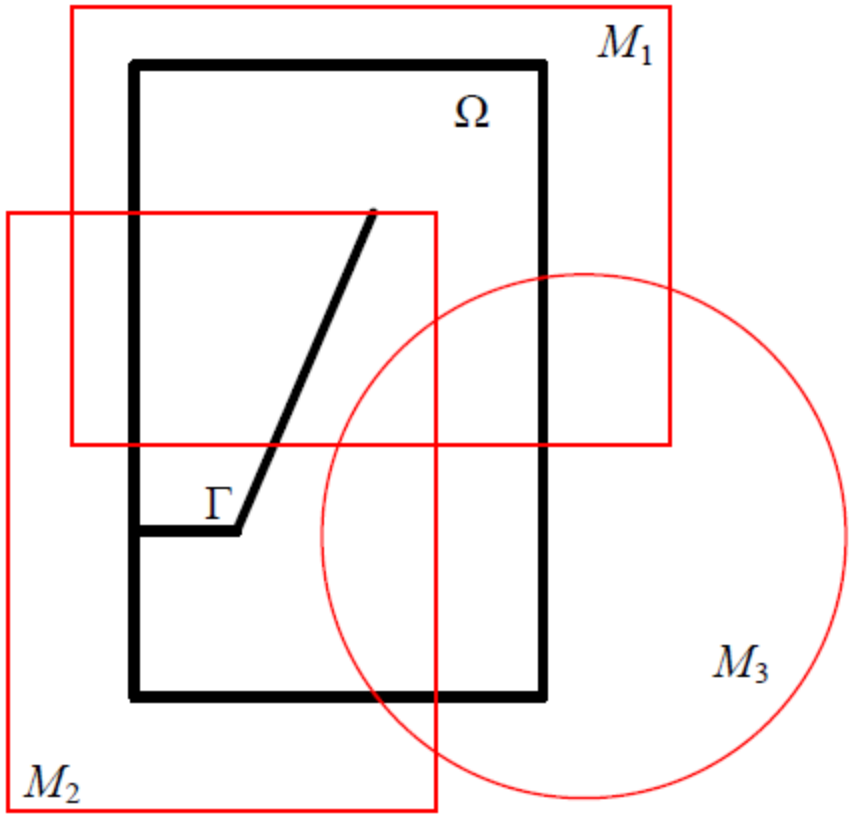

Fig. 2. Problem domain Ω containing a crack Γ (thick black lines) and MC (red lines)

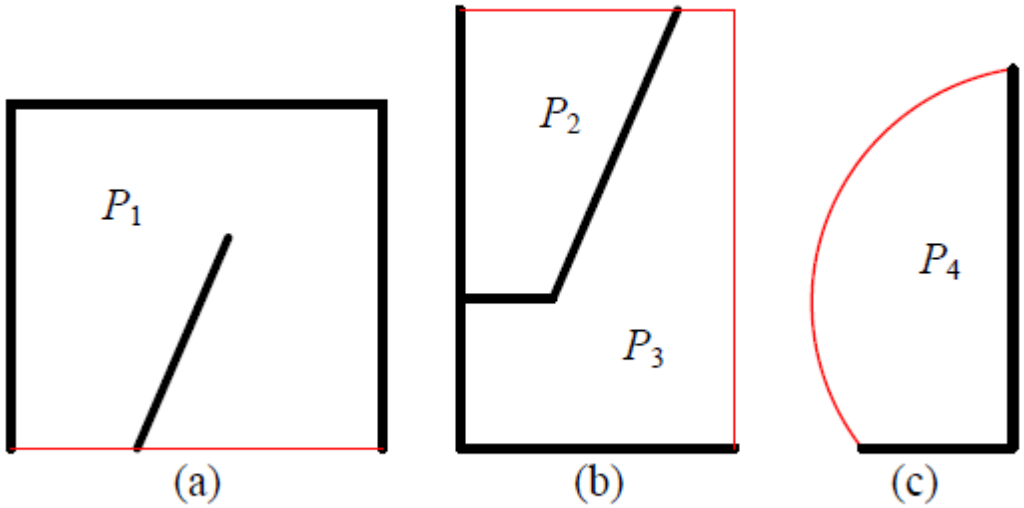

Fig. 3. Physical patches

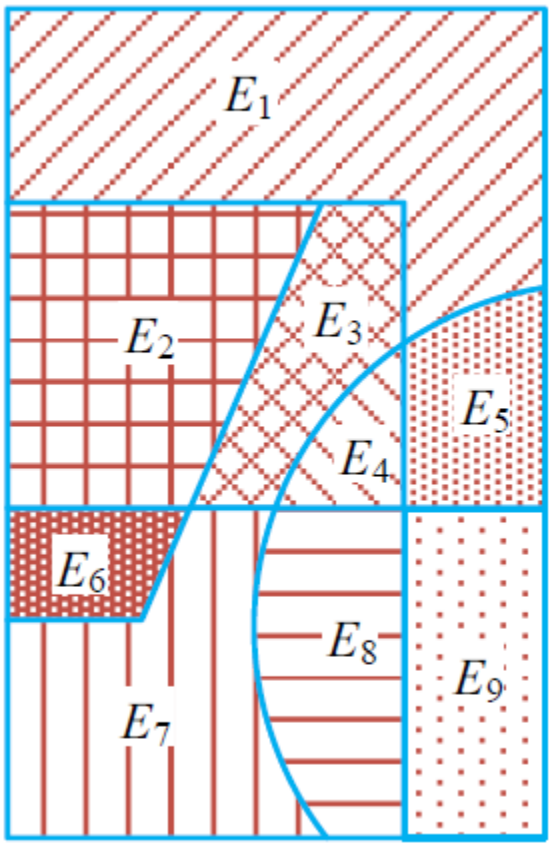

Fig. 4. Manifold elements from E_1 to E_9.

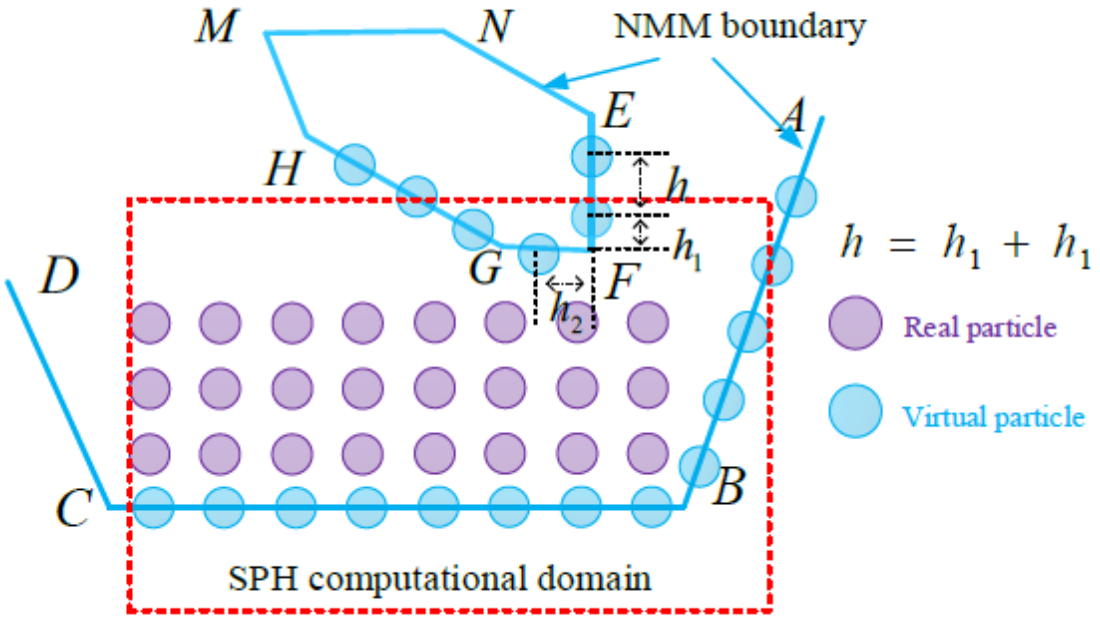

Fig. 5. The computational domain of SPH and the Layout of virtual particles

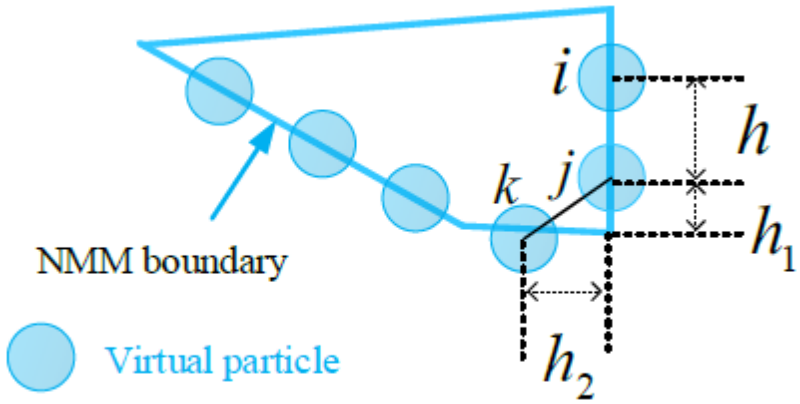

Fig. 6. The distribution of virtual particles on the NMM boundaries. *h* is the original distance of real particles, $h=h_1+h_2$

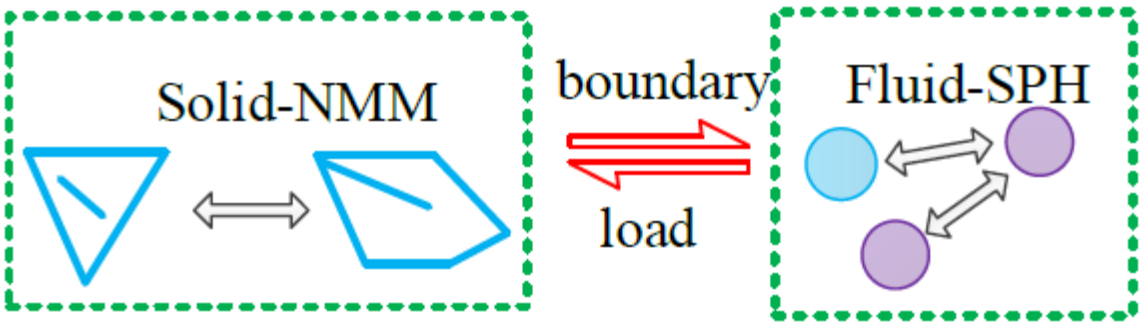

Fig. 7. The interaction scheme of the coupled NMM-SPH method.

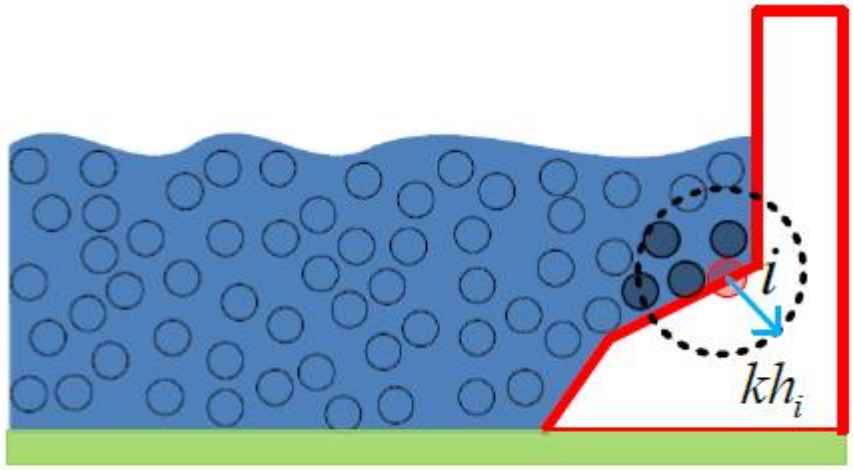

Fig. 8. Compute the pressure of virtual particles.

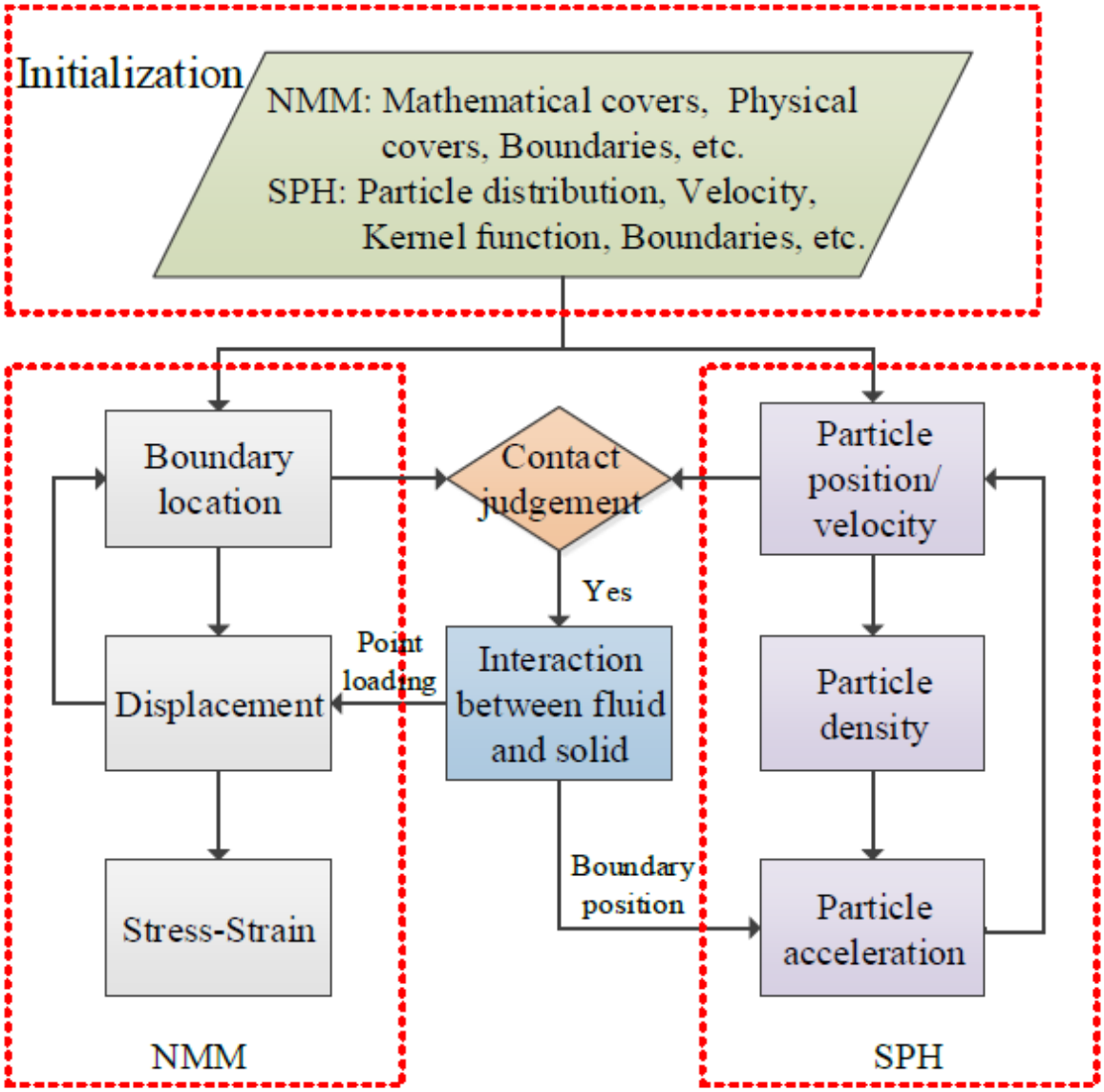

Fig. 9. Computation process of the coupled NMM-SPH method.

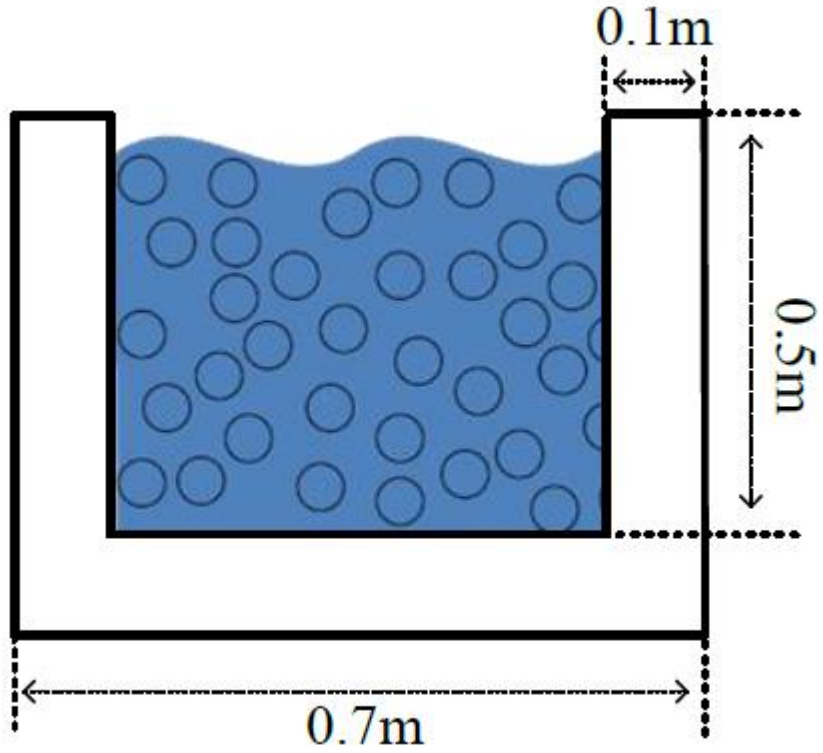

Fig. 10. Hydrostatic pressure test.

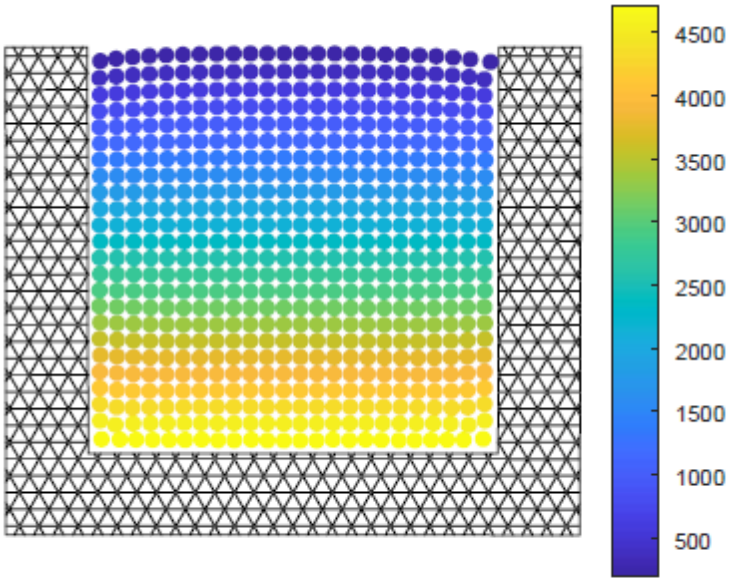

Fig. 11. Final configuration and hydrostatic pressure.

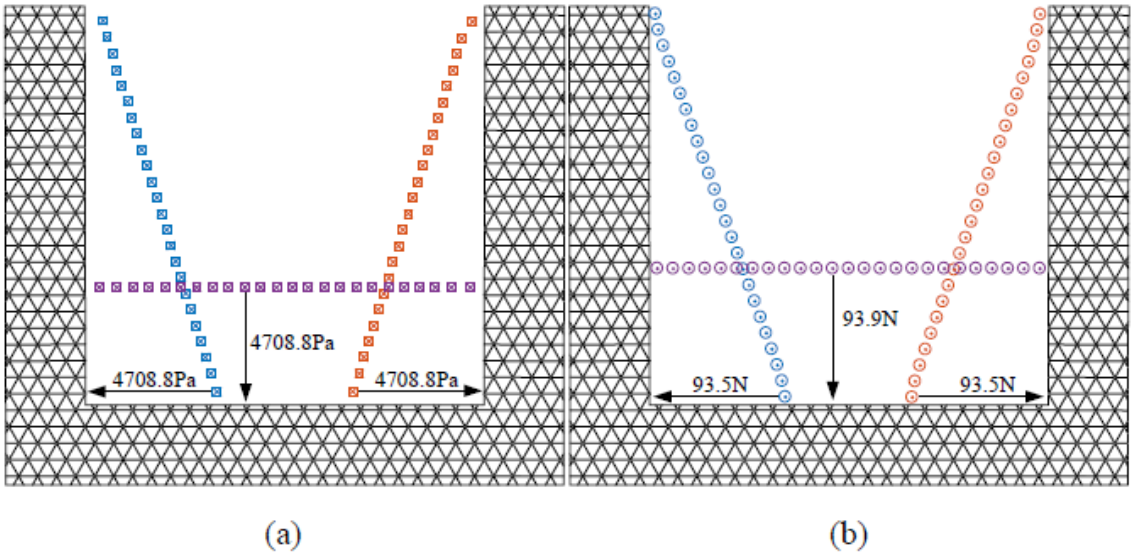

Fig. 12. Results from NMM-SPH, (a) water pressure of particles along the internal boundaries;(b)point loading of virtual particles.

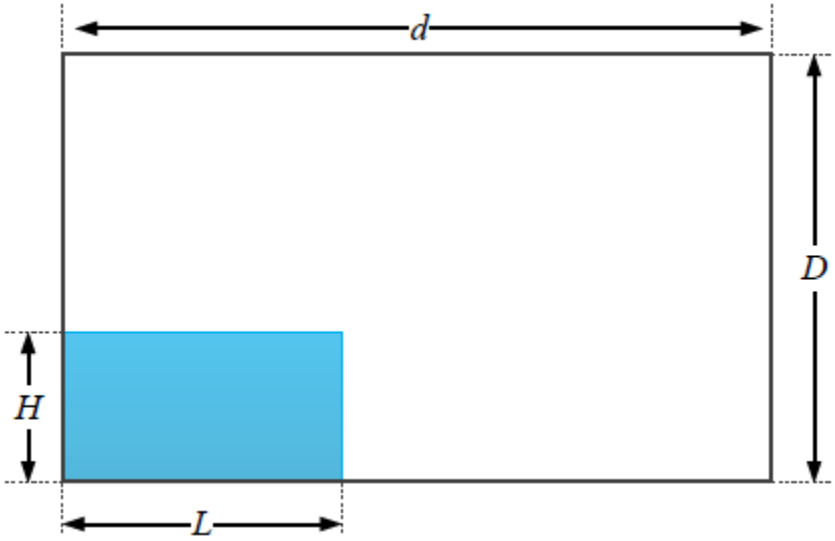

Fig. 13. Definition of the dam-break problem. A rectangular patch of water is initially at rest behind a wall. *H* is the height of the water column, *L* is its length, *d* is the length of the rectangular box that contains the fluid and *D* is its height.

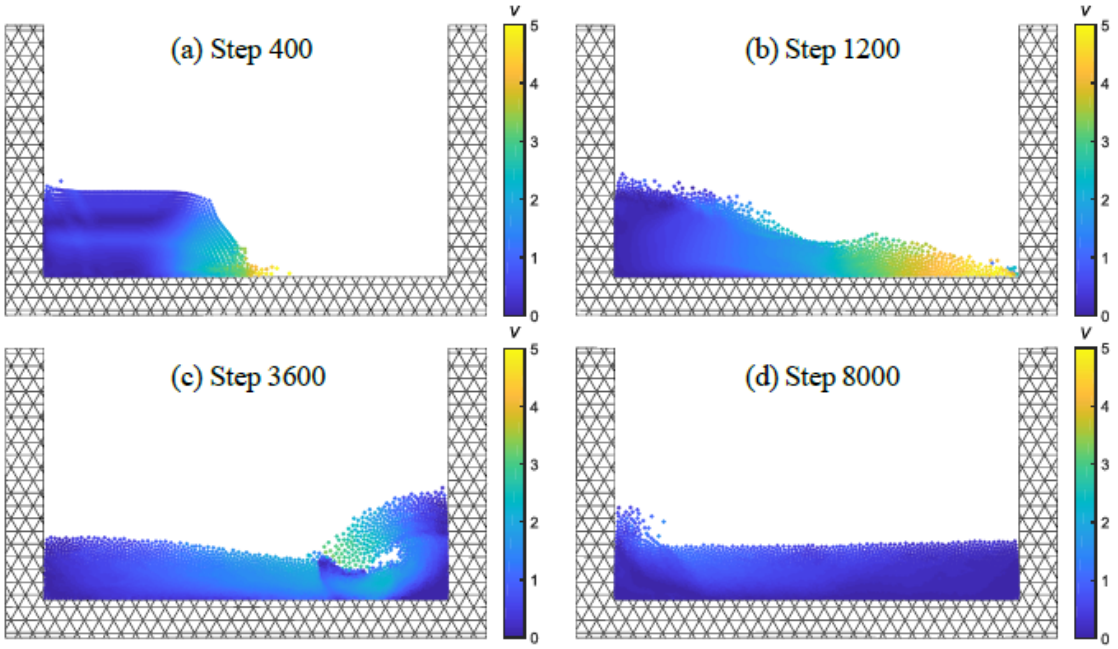

Fig. 14. Time evolution of the water domain after the dam breaking.

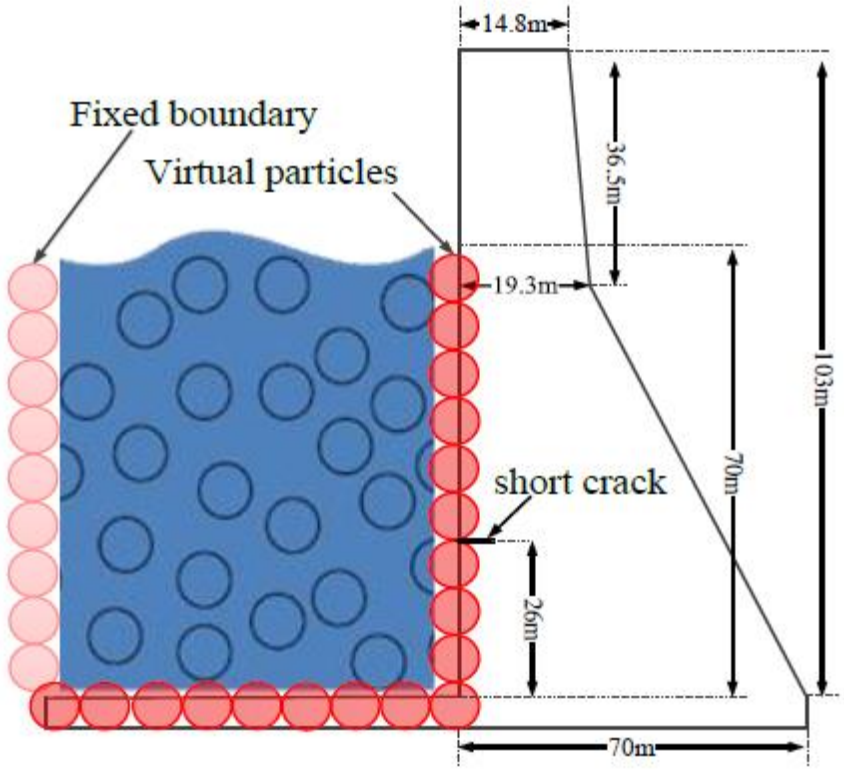

Fig. 15. The initial configuration of the dam with a short crack.

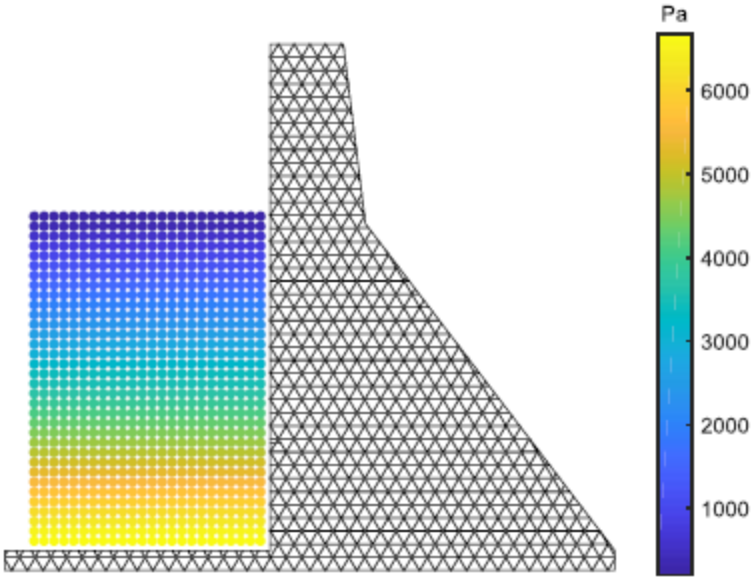

Fig. 16. The initial arrangement of NMM mesh and SPH particles (with initial hydraulic pressure).

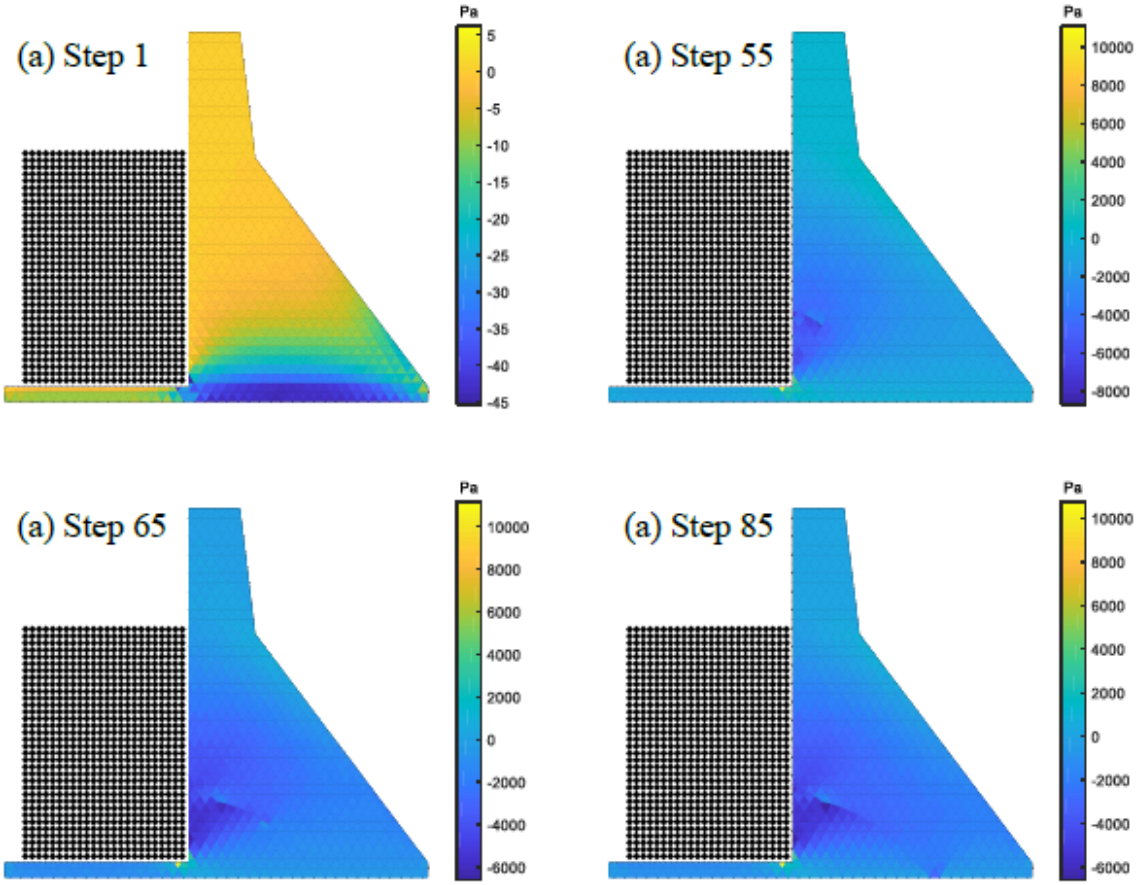

Fig. 17. The crack paths and the stress in x-direction of the dam at different steps.